Pergamon

Chaos, Solitons & Fractals Vol. 4, Nos 8/9, pp. 1683–1698, 1994

0960–0779/94$7.00 + .00

0960–0779(94)E0040–V

Multistability and Periodic Alternance in a Multimode CO_2 Laser with a Saturable Absorber

D. WILKOWSKI, D. HENNEQUIN, D. DANGOISSE and P. GLORIEUX

Laboratoire de Spectroscopie Hertzienne, Unité associée au Centre National de la Recherche Scientifique (URA 249), Université des Sciences et Technologies de Lille, F-59655 Villeneuve d'Ascq cedex, France

Abstract—The transverse dynamics of a multimode CO_2 laser with SF_6 as an intracavity saturable absorber is experimentally studied. Generalized multistability, periodic alternance and passive Q-switching involving several laser transverse modes have been observed. The dynamics is more particularly studied in the simplest case of the bimode laser where antiphase and in-phase self-oscillations are obtained. In the highly multimode case, experimental conditions are found in which the absorber acts as a mode filter that reduces complex transverse patterns to almost pure Hermite–Gauss modes.

INTRODUCTION

In the past few decades, the laser with saturable absorber (LSA) has received much interest in relation to its strong potential applications in laser physics. This system, even in its monomode regime, exhibits a large variety of behaviours and shows, for example, spontaneous instabilities referred to as passive Q-switching (PQS). These instabilities have been understood in relation to the existence of a homoclinic orbit in the phase space, and Shilnikov chaos has been clearly evidenced both theoretically and experimentally [1–3]. Depending on the experimental conditions, bistability has also been found between the stationary on and off states as well as between different PQS regimes [4].

All these studies dealt with singlemode LSAs and very few works considered the multimode operation of this system [5]. As long ago as 1968, Chebotayev and coworkers [6] observed that the LSA could display 'spectral hysteresis' together with the more common power hysteresis. They also pointed out the ability of the LSA to filter weak longitudinal modes. The use of an intracavity saturable absorber was also proposed to filter out weak *transverse* modes appearing in the far-off axis region of a laser beam.

More recently, transversally multimode regimes of lasers and optical oscillators have been reinvestigated experimentally in the framework of the development of nonlinear dynamics in the field of laser physics [7–13]. As a first step, the investigations on multimode laser dynamics adopted a global approach in which the spatial dependence was not explicitly introduced [14]. Later, the theory included all the cavity modes and Lugiato *et al*. studied the interaction between the modes belonging to the same frequency-degenerate family. They predicted spontaneous symmetry-breaking, a phenomenon which was observed experimentally on the TEM_{01} and TEM_{10} modes of the Na_2 laser by Tamm and Weiss [9]. Using a CO_2 laser cavity with an intracavity telescope, Tredicce *et al*. showed that the transverse mode spacing plays a crucial role in the nonlinear interaction of transverse cavity modes [13]. In particular they found that cooperative frequency-locking occurs only when the modes have nearly degenerate frequencies, a result that reproduced the early predictions and observations of Rosanov *et al*. on He–Ne lasers [15]. Interaction

between different transverse modes was also studied in these lasers by Auston and Smith, but with a different point of view [16, 17]. In all the above-mentioned studies, the modal expansion of the electric field is valid but, as the Fresnel number becomes large, an 'hydrodynamical' approach is required. The patterns observed in this case are interpreted as arising from the formation of 'optical vortices'. This is the case of recent studies on photorefractive oscillators [11, 12] in which periodic alternance, quasiperiodicity and chaotic itinerancy have also been observed.

In the particular case of the LSA, special attention has been paid to the 2-mode situation. The dynamics of the bimode laser can obey the Farey arithmetics [18, 19]. A transition from quasiperiodicity to chaos has also recently been observed in the bimode CO_2 + SF_6 LSA [20]. Moreover, Tachikawa *et al.* [21, 22] investigated the similar problem in the case of the coupling of two different laser lines in the CO_2 LSA. All these works are related to the general problem of interaction between oscillators that is also encountered in other domains such as electronics [23], biology [24] and chemistry [25].

The aim of this paper is to present experimental results on the CO_2 LSA in which the transverse pattern dynamics is explicitely considered. Contrary to previous works in which the interaction between modes was considered from a general point of view, here the transverse pattern dynamics is resolved and considered *per se*. This situation is considered numerically by Arimondo *et al.* in [26]. The transverse modes involved are mostly the low order Hermite–Gauss or Laguerre–Gauss modes, except in the last part of this paper. All through this study, we have used a specially designed CO_2 laser with large transverse dimensions in which the degree of mode interaction could be controlled. Depending on the operating conditions of this laser, generalized multistability and periodic alternance between laser modes could be observed. In particular, generalized multistability has been observed in very different situations between stationary states, or dynamical and stationary states as well as between different dynamical regimes. As was proposed by C. O. Weiss [10], laser multistability is of great interest for pattern recognition.

The present report is organized as follows. After a brief description of the experimental set-up, we analyse the different cw and dynamical regimes obtained in a bimode laser both with a pure absorber and with addition of a buffer gas. Then the evolution of the different regimes is studied as a function of the absorber pressure and the cavity detuning. This study is later extended to weakly multimode regimes in which the role played by the cavity symmetry breaking due to, for example, Brewster windows, is emphasized. Finally, we give an overview of the patterns observed in the LSA involving high-order modes.

EXPERIMENTAL SET-UP

The system considered here is a CO_2 laser with large transverse dimensions, containing an intracavity cell filled with SF_6 at low pressure acting as a saturable absorber.

Two different cavities have been used that differ only by the value of their maximum Fresnel number N_{max} which reaches 10 for the first cavity and 37 for the second (Fig. 1). Both cavities are limited by a concave mirror which acts as an output coupler with reflectivity of 0.95, and a grating tuned on the 10P20 or 10P16 lines to keep the laser emission in coincidence with the strongest gas absorptions. The corresponding SF_6 absorption lines differ by both the absorption coefficient and the detuning from the centre laser frequency. However, the effects observed on both lines are qualitatively the same and, unless otherwise specified, the experimental results reported in this paper were obtained with a CO_2 laser operating on the 10P20 line.

The first cavity whose length is 1.7 m has thereby a free spectral range $\Delta\nu_L = 88$ MHz

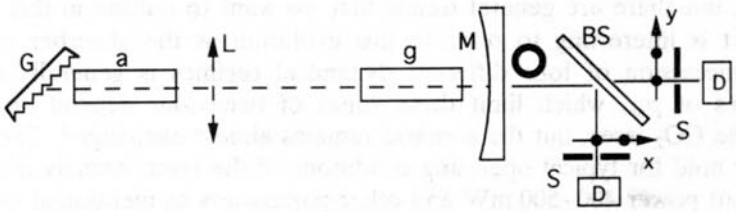

Fig. 1. Experimental setup: G = grating, L = lens, M = mirror, BS = beam splitter, S = stop, a = absorber medium, g = gain medium. The experimental parameters are: active medium ($1 < A < 2$, line: 10P20 or 10P16 with $\Delta\nu_H = 350$ MHz), saturable absorber ($\Delta\nu_D = 30$ MHz), cavity [$\Delta\nu_L = 88$ MHz, $\Delta\nu_T = 17$ MHz, $N_{max} = 10$ (without intracavity lens) or 37 (with lens)].

and a transverse intermode spacing $\Delta\nu_T = 17$ MHz fixed by the 5 m radius of curvature of the output coupler. In the second cavity the output coupler has a 1 m radius of curvature and a positive lens with a focal length of 600 mm has been introduced inside the cavity. Slight displacements of the lens position would allow us to vary the transverse mode spacing if necessary. The two cells containing the amplifier and the absorber are closed by Brewster windows that introduce a strong astigmatism in the cavity and lift the frequency degeneracy inside the transverse mode families. However, in order to vary the symmetry properties of the cavity, the Brewster windows can be partially or totally replaced by antireflection (AR) coated plates. In order to avoid formation of coupled cavities inside the laser, the AR plates are slightly tilted with respect to the cavity axis. The degeneracy lift inside a family of quasidegenerate modes can be slightly modified in the range 0–4 MHz by changing the number of Brewster windows. In this case the residual asymmetry is induced by misalignment or by defects in the optical components of the cavity.

The active medium, a mixture of CO_2, N_2 and He (in the proportion of 1:1:3) at a total pressure of 70 Torr, is homogeneously broadened ($\Delta\nu_H = 350$ MHz). On the contrary, the saturable absorber SF_6 is introduced only at low pressure ($1 < p_{abs} < 30$ mTorr) and is inhomogeneously broadened ($\Delta\nu_{Doppler} = 30$ MHz). The length of the active (resp. absorbing) cell is 70 cm (resp. 25 cm). Helium used as a buffer gas has been added to SF_6 in variable amounts ($1 < p_{total} < 300$ mTorr). In fact, the parameter domain reached by the mixture (SF_6 + He) is noticeably different from that corresponding to CH_3I used in our previous study [16] since SF_6 has larger absorption coefficient and saturability and the addition of He in the absorber allows us to go from the case of an inhomogeneously broadened absorber (low pressure pure SF_6) to an almost homogeneously broadened one (high He pressure).

We have measured both the total intensity as displayed by thermal plates and the local intensity in a given part of the beam using a fast HgCdTe detector. During the study of the bimode laser operating on the TEM_{01} and TEM_{10} modes, two fast detectors have been set in such a way that they could follow the evolution of the signal emitted by each mode individually (Fig. 1). The accessible control parameters in these measurements are the pressures of the active and passive media, the intensity of the laser discharge, the tuning of the cavity length and the Fresnel number that can be adjusted by means of an iris. As far as the spectrum of the empty cavity modes is concerned, the spacing between transverse families is fixed in cavity 1 but can be adjusted in cavity 2.

OVERVIEW OF THE MULTIMODE BEHAVIOUR OF THE LSA (PURE SF_6)

The dynamical regimes of the LSA described above have been explored in a wide range of variation of the control parameters. A great variety of spatio-temporal behaviours have

been observed, but there are general trends that we want to outline in this paragraph. To that purpose, it is interesting to refer to this evolution as the absorber pressure p_{abs} is increased. A succession of four different dynamical regimes is generally observed. The particular values of p_{abs} which limit these zones of behaviour depend on the operating conditions of the CO_2 laser, but the scenario remains almost unchanged. The values of p_{abs} given hereafter hold for typical operating conditions of the laser, namely discharge current 5–10 mA, output power 400–500 mW and other parameters as mentioned in the preceding section.

(1) At low SF_6 pressures ($0 < p_{abs} < 5$ mTorr), the absorber plays a negligible role and the dynamics of the system resembles that of the CO_2 laser without absorber [27].

(2) For intermediate SF_6 pressures ($5 < p_{abs} < 10$ mTorr), mode oscillation is now ruled by periodic alternance between all the transverse modes allowed to oscillate. Different switching sequences have been obtained depending on the experimental conditions.

(3) If the pressure is further increased ($10 < p_{abs} < 15$ mTorr), a new domain is reached where the laser exhibits multistability between singlemode and stationary states. The corresponding singlemode outputs appear to be very similar to pure Hermite–Gauss modes of the empty cavity. It has been observed that the number of stationary states involved in the multistability depends obviously on the location of the mode families inside the gain curve, and may reach a value of 10 with a Fresnel number fixed at $N = 10$. The width of the multistability window depends also on the pump parameter A and is maximum for $A = 1.2$. It has been observed experimentally that multistability between stationary states disappears completely above $A = 1.5$ whatever the number of modes having positive gain.

(4) When the pressure is fixed in the range 15–20 mTorr, the laser exhibits PQS as it is commonly observed in a monomode LSA, but here many modes are simultaneously involved in a more complex way. Winner-Takes-All dynamics with antiphase oscillation of two or three modes is typically obtained, but other kinds of time evolution may be observed. Finally, laser emission stops above $p_{abs} = 20$ mTorr typically.

This behaviour is quite general, and does not depend critically on the number of interacting modes. Another general observation is that, as mentioned above, the transverse patterns delivered by our LSA in singlemode operation are very close to Hermite–Gauss modes of the empty cavity. The fact that pure modes are delivered by the active laser is not surprising, because both the gain and the refractivity of the medium remain small due to the low transmission of the output coupler and the dilute character of the active medium. Therefore, the Hermite–Gauss basis will be extensively used in the following sections. In this description, the modes are labelled TEM_{mn} with indices m and n refering to the vertical and horizontal axes. The resonance frequencies of these modes cluster into subsets (families) labelled by the order $q = m + n$ [8]. After this overview, let us now be more specific and illustrate in more detail the simplest case of the bimode laser.

TWO-MODE DYNAMICS (PURE SF_6)

This investigation was carried out at both low pump parameter ($A = 1 - 1.4$) and moderate Fresnel number ($N = 3$–5). In these conditions, only a few families ($q = 0, 1, 2$) may be individually selected through the resonator length and their overlapping domains are very narrow. First, we have studied the simplest situation in which only the two modes TEM_{01} and TEM_{10} belonging to the family $q = 1$ are activated. Patterns arise from intermodal interaction inside both the active and passive media. The transverse patterns observed in the LSA are so close to the empty cavity modes that we will use hereafter the Hermite–Gauss terminology to describe them.

When operated in the bimode (TEM_{01} and TEM_{10}) regime, the LSA exhibits successively the four regimes described in the preceding section. We give in the following a more detailed description of these spatiotemporal dynamics (Fig. 2).

(1) At low SF_6 pressures, an unlocked bimode regime is observed where the two modes are simultaneously oscillating, and the resulting averaged pattern of the laser is a doughnut (Fig. 3). The temporal signature of this regime is the beating of the total intensity at the intermode frequency, here 2.4 MHz when the laser is operated with four Brewster windows. This mode splitting results from the degeneracy lift due to the astigmatism of the cavity. Different optical paths for the two modes due to astigmatism were also found in a conventional CO_2 laser without saturable absorber were such beatings are commonly observed [27].

(2) At increasing pressures in the absorber ($p_{abs} = 5$ mTorr typically) this regime of mode-beating stops and is replaced by a regime of periodic alternance between the same two modes. In such a regime, the two modes oscillate alternatively with a period much longer than the beating period of the previous regime (Fig. 4). This alternance occurs at a low repetition rate (1–2 kHz typically) which decreases with SF_6 pressure and tends to zero

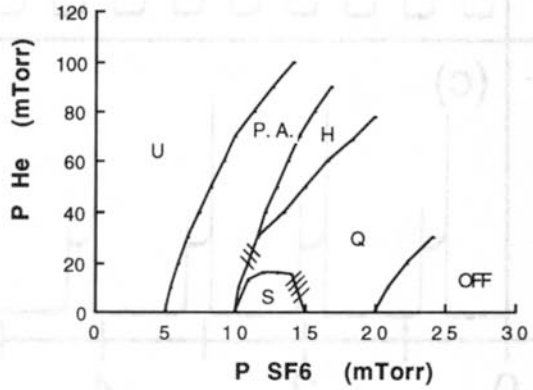

Fig. 2. Phase diagram of the LSA in the bimode (TEM_{01} and TEM_{10}) regime as a function of both SF_6 and He pressure in the absorber cell. U = unlocked doughnut, S = time independent (bistable) regimes, P.A. = periodic alternance and Q = in-phase Q-switch, H = irregular regimes of hesitation between periodic alternance and in-phase Q-switch.

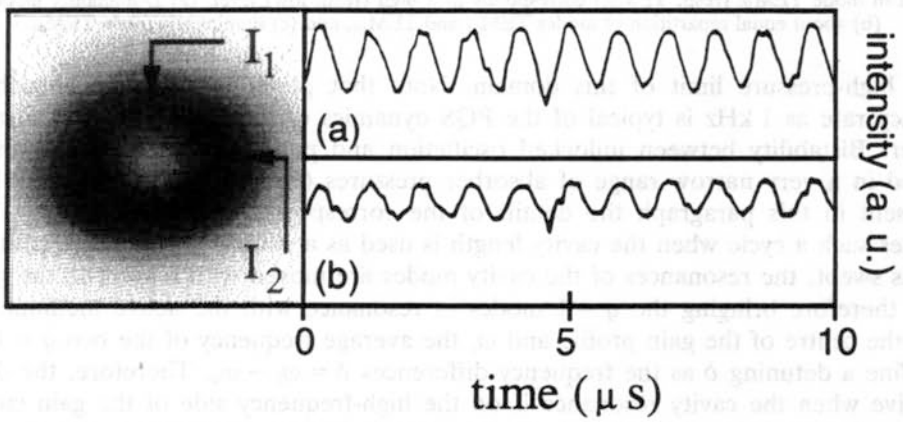

Fig. 3. Unlocked regime in the $q = 1$ family. (Left) Time-average transverse pattern of the laser emission. (Right) Time-evolution of the intensity detected by the two detectors located as indicated on the left side pattern.

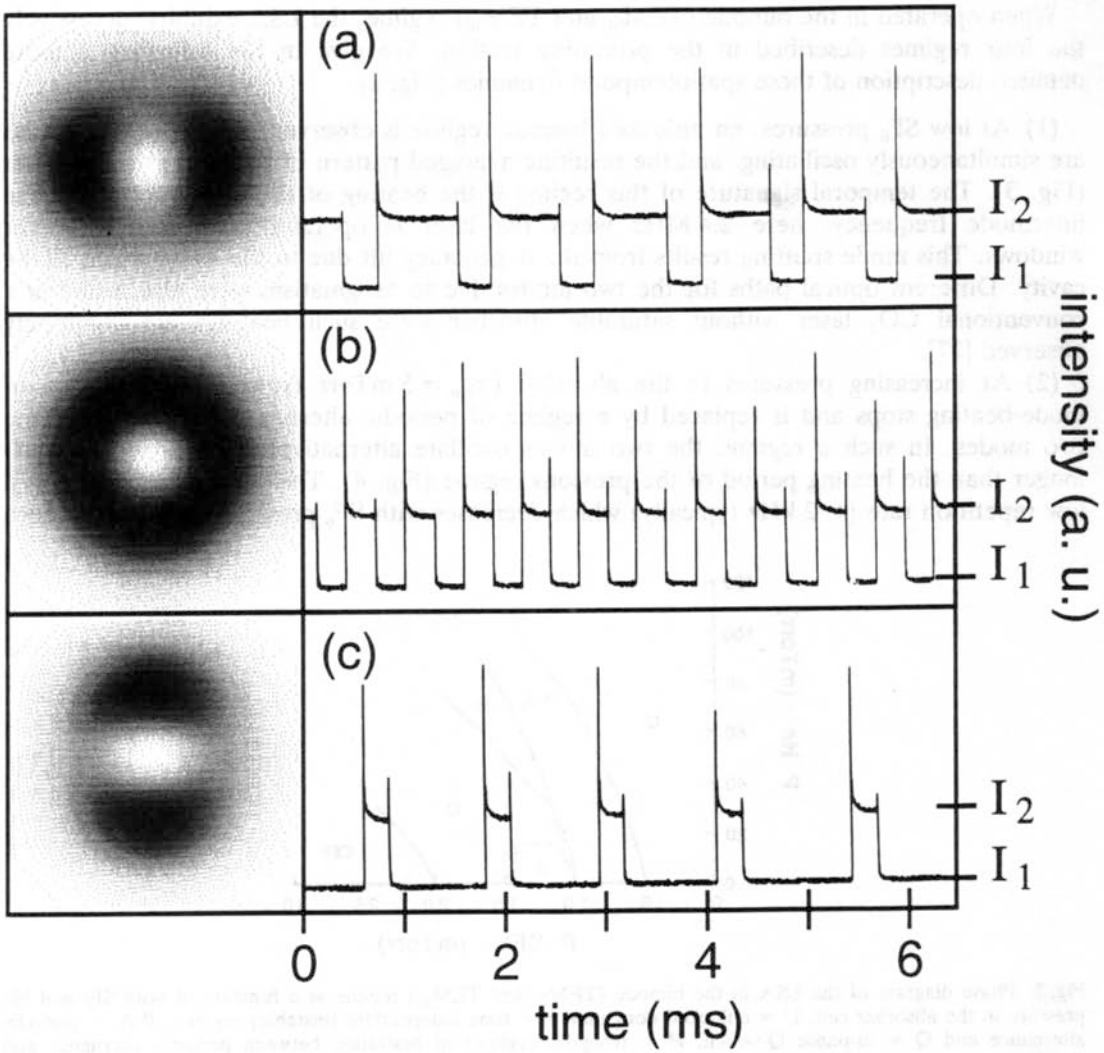

Fig. 4. Periodic alternance between the TEM_{01} and TEM_{10} modes for different values of the cavity detuning. (Left) Time-averaged patterns. (Right) Time-resolved variation of the intensity. The detector is located such that oscillation in mode TEM_{10} (resp. TEM_{01}) corresponds to a high (resp. low) level. (a) Dominantly mode TEM_{01}, (b) about equal repartition of modes TEM_{01} and TEM_{10}, and (c) dominantly mode TEM_{01}.

on the high-pressure limit of this domain. Note that periodic switching at such a low frequency rate as 1 kHz is typical of the PQS dynamics of the CO_2 laser with a saturable absorber. Bistability between unlocked oscillation and periodic alternance has also been observed in a very narrow range of absorber pressures ($5 < p_{abs} < 7$ mTorr typically) and we present in this paragraph the details of the corresponding hysteresis cycle. Figure 5 illustrates such a cycle when the cavity length is used as a control parameter. As the cavity length is swept, the resonances of the cavity modes are moved with respect to the gain-line centre, therefore bringing the $q = 1$ modes in resonance with the active medium. Let us call ω_a the centre of the gain profile and ω_1 the average frequency of the two $q = 1$ modes and define a detuning δ as the frequency differences $\delta = \omega_1 - \omega_a$. Therefore, the detuning is positive when the cavity resonance is on the high-frequency side of the gain curve and negative when it is on the other side. To observe modal bistability, a return sweep is performed from $-\delta_0$ to $+\delta_0$ with δ_0 positive and such that the mode families $q = 0$, 1 and

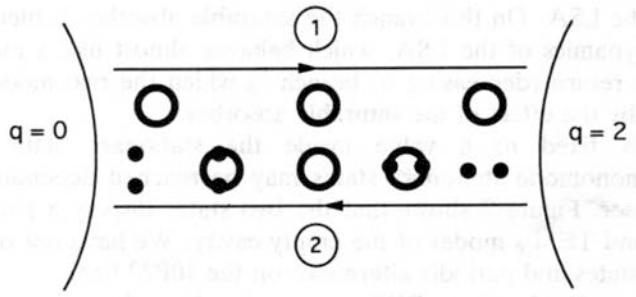

Fig. 5. Bistability between (1) unlocked doughnut and (2) antiphase states in the $q = 1$ family with cavity length as a control parameter.

2 are successively brought into resonance with the gain line. When the laser switches from the TEM_{00} mode (i.e. $q = 0$) to the $q = 1$ family, the two modes (TEM_{10} and TEM_{01}) are first simultaneously activated and oscillate freely with a frequency difference of 2.4 MHz. The time-averaged pattern appears as a regular doughnut with a shape independent of the detuning. When the detuning is increased, both modes remain present until a large positive detuning situation is reached so that the laser switches to the $q = 2$ family. When the detuning is progressively decreased from δ_0 to $-\delta_0$, the laser switches from the $q = 2$ to the $q = 1$ family, but the pattern is continuously changing from the TEM_{10} mode to the TEM_{01} mode. The LSA is then in a regime of periodic alternance in which it switches periodically from one transverse pattern to the other with cyclic ratio depending on the detuning δ. In this situation, the beating at 2.4 MHz disappears because the modes never oscillate simultaneously. On the thermal plate, the average pattern becomes an irregular doughnut showing clearly which of the two modes (i.e. TEM_{01} or TEM_{10}) has the largest duration of oscillation. The cyclic ratio R_T is defined as the relative emission duration of the mode TEM_{10} as compared to period of the signal. R_T is a function of the cavity detuning and may vary continuously from 0 (pure TEM_{01}) to ∞ (pure TEM_{10}). Figure 6 illustrates the typical evolution of this cyclic ratio as a function of the detuning for a fixed value of the absorber pressure in the range corresponding to periodic alternance ($p_{abs} = 12$ mTorr) in the case of the 10P16 CO_2 line. It shows the continuous character of the transition from one transverse pattern to the other. The two branches of the hysteresis cycle have a completely different character. The fact that the increasing δ branch is similar to the unlocked dynamics of the CO_2 laser is reminiscent of the high power branch of the

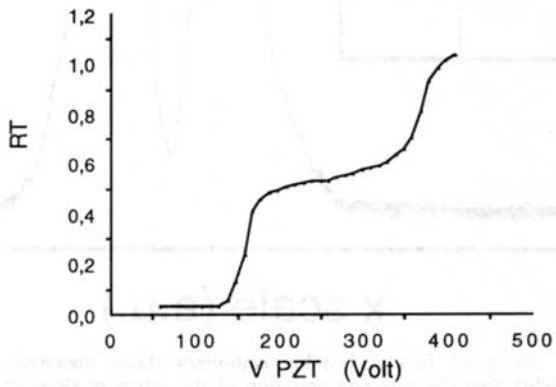

Fig. 6. Variation of the cyclic ratio of periodic alternance regime as a function of the cavity detuning.

bistability cycle of the LSA. On this branch the saturable absorber is bleached, and plays a minor role in the dynamics of the LSA, which behaves almost like a pure CO_2 laser. On the other hand, the return (decreasing δ) branch in which the two modes are pulsating is strongly dominated by the effect of the saturable absorber.

(3) When p_{abs} is fixed to a value inside the stationary state range ($10 < p_{abs} < 15$ mTorr), two monomode stationary states may be reached depending on the starting conditions of the laser. Figure 7 shows that the two states display a pattern very close to that of the TEM_{01} and TEM_{10} modes of the empty cavity. We have not observed bistability between stationary states and periodic alternance on the 10P20 line.

(4) When p_{abs} exceeds 15 mTorr, PQS appears in which the two modes emit in-phase PQS pulses. The period of Q-switching decreases with the absorber pressure. As in the monomode regime, the signal emitted in each mode is composed of a large spike followed

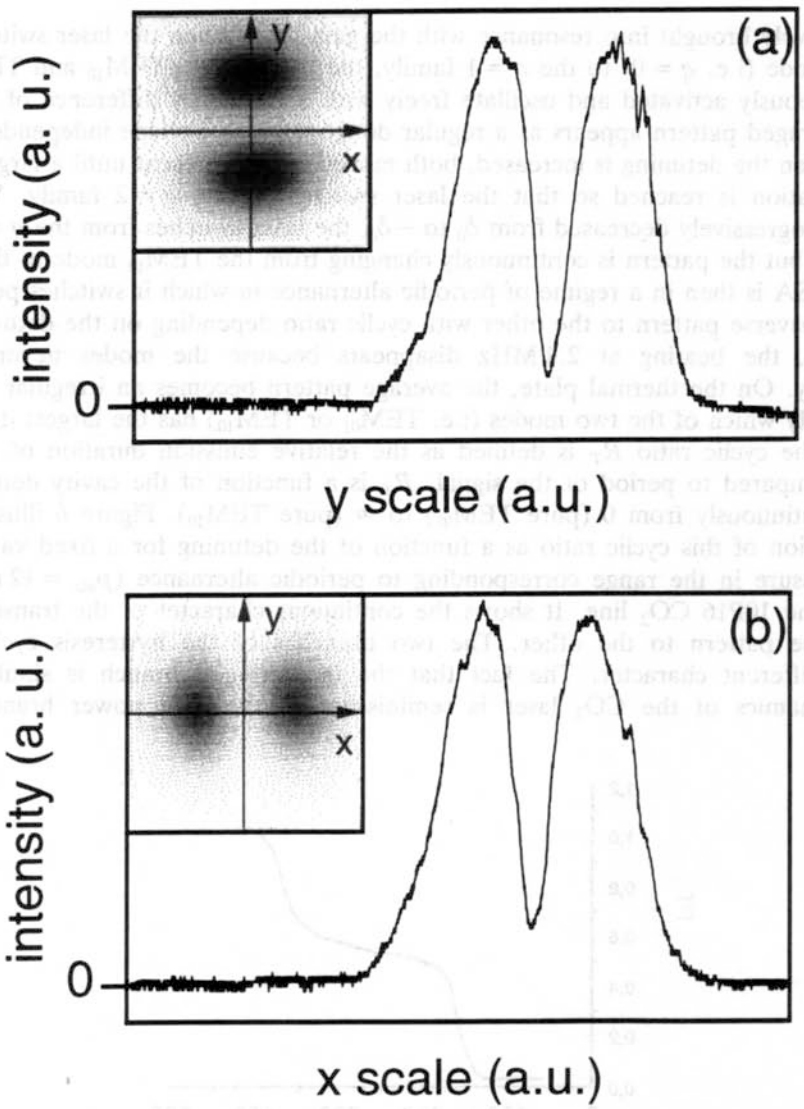

Fig. 7. Stationary states of the $q = 1$ family: bistable stationary states observed at $P_{abs} = 12$ mTorr. (Left) Time-averaged patterns. (Right) Spatially resolved variation of the intensity along the y (resp. x) direction. (a) TEM_{01}, (b) TEM_{10}.

by a slow decrease towards a quasistationary value. Before this limit is actually reached, oscillations of exponentially increasing amplitude destabilize the system until emission stops. Such destabilization through increasing oscillations is a common feature of the $CO_2 + SF_6$ monomode LSA [4, 20]. However, this Q-switching regime is completely different from the periodic alternance discussed above, that is, the amplitude of the two modes oscillate in-phase as shown on Fig. 8. Three very different time scales are present in these signals. The lowest scale (a few ms) governs the period of the PQS [Fig. 8(a) and (b)]. The intermediate one corresponds to the period of the oscillations that appear in the PQS [Fig. 8(c) and (d)]. As the two modes oscillate in phase, a beating at their frequency difference is superimposed on the Q-switching signal [Fig. 8(e) and (f)]. Therefore, this

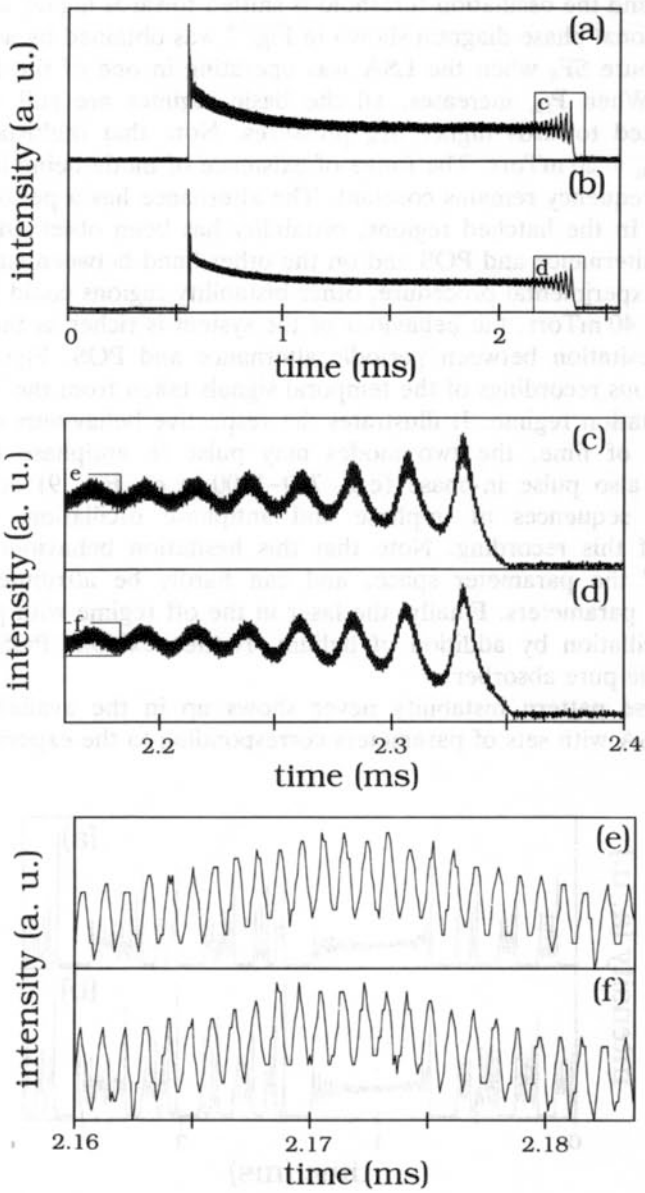

Fig. 8. Q-switching in a bimode LSA. (a): TEM_{10}, (b): TEM_{01}. The inserts (c)–(f) show time-expanded versions of these signals with increasing magnification.

regime is characterized by the simultaneity of mode-beating and PQS. Bistability between PQS and stationary states has been observed in our set-up in the vicinity of $p_{abs} = 15$ m-Torr. Moreover, bistability between PQS where the modes oscillate in phase and periodic alternance has also been found in the parameter domain when the stationary state window is suppressed by increasing the pump parameter A above 1.5.

TWO-MODE DYNAMICS (SF_6 + He)

The accessible parameter range may be extended by adding He as a buffer gas to SF_6. When the partial pressure p_{He} of He is increased, the homogeneous broadening of the medium increases and the oscillation threshold is shifted towards higher absorber pressures.

The two-dimensional phase diagram shown in Fig. 2 was obtained by adding adiabatically the buffer gas to pure SF_6 when the LSA was operating in one of the four basic regimes discussed above. When P_{He} increases, all the basic regimes are still observed, but are systematically shifted towards higher SF_6 pressures. Note that multistability is no more observed above $p_{He} = 20$ mTorr. The range of existence of mode being increases with p_{He}, but obviously its frequency remains constant. The alternance has a period which decreases with He pressure. In the hatched regions, bistability has been observed on the one hand between periodic alternance and PQS and on the other hand between stationary states and PQS. Due to the experimental procedure, other bistability regions could have been missed. When p_{He} exceeds 40 mTorr, the behaviour of the system is richer as there appears a new domain (H) of hesitation between periodic alternance and PQS. Figure 9 shows as an example simultaneous recordings of the temporal signals taken from the TEM_{01} and TEM_{10} modes in this hesitation regime. It illustrates the respective behaviours of the two modes. For some periods of time, the two modes may pulse in antiphase (e.g. 0–600 μs on Fig. 9), they can also pulse in-phase (e.g. 700–1400 μs on Fig. 9) or they can display apparently erratic sequences of in-phase and antiphase oscillations as shown in the 1.5–2.2 ms part of this recording. Note that this hesitation behaviour is obtained in a significant part of the parameter space, and can hardly be attributed to the lack of stabilization of the parameters. Finally, the laser in the off regime with pure absorber may be brought to oscillation by addition of helium. It then exhibits PQS but at a smaller period than with the pure absorber.

As the transverse pattern bistability never shows up in the available models of the multimode CO_2 LSA with sets of parameters corresponding to the experimental conditions,

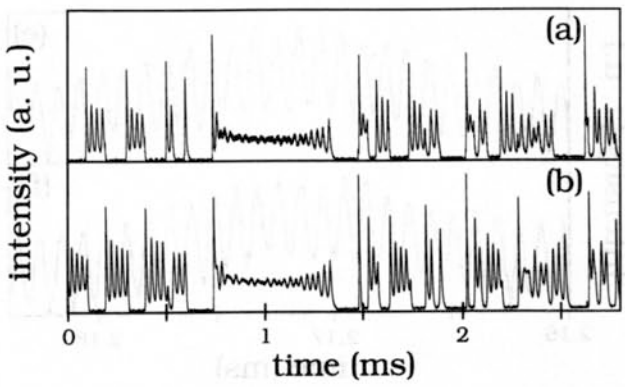

Fig. 9. Simultaneous recordings of irregular regimes in the LSA when He is added to the absorber. (a): TEM_{01} mode, (b): TEM_{10} mode. For experimental conditions, see Fig. 2.

it is interesting to explore the parameter space in order to determine what is the physical origin of this effect. It appears first that the amplitude of the mode-degeneracy lift plays a key role. For instance, when the spacing between the transverse modes is reduced from 2.4 MHz to 1.2 MHz by replacing two of the four Brewster windows by AR plates, the region of pattern bistability completely disappears. However, bistability may be reobtained as a small asymmetry is introduced in the cavity, for example, by slighty misaligning it. The second key parameter is the homogeneous broadening of the absorber. Adding helium to the saturable absorber changes mostly its homogeneous linewidth. Figure 2 also shows that bistability suffers from the introduction of helium in a quite different way from the other dynamical regimes since it cancels completely the bistability domain while it only shifts the boundaries of the domains in which the other regimes are observed. The interplay of homogeneous broadening and mode degeneracy lift by asymmetry may be interpreted as follows. When the asymmetry between the TEM_{01} and TEM_{10} modes is relatively large, leading, for example, to a mode degeneracy lift of 2.4 MHz, which is significantly larger than the homogeneous broadening of the saturable absorber (about 300 kHz), these two modes can burn two holes in the velocity distribution corresponding to two nonoverlapping velocity groups. However, when the asymmetry is reduced, the mode splitting decreases and the laser radiation interacts with non-independent velocity groups, leading to a stronger competition between the two modes.

MULTIMODE DYNAMICS

Bimode dynamics of the LSA can serve as a basis to understand the multimode dynamics. Somehow unexpectedly, the general multimode behaviour remains very similar to the bimode case in the experiments carried out with a pure SF_6: the four regimes described above are again found as the absorber pressure is varied. For example, Fig. 12 shows the output of the HgCdTe detector in a three-mode regime of periodic alternance. As the whole beam is focused on the detector, the intensity never falls to zero. If we ignore the spikes corresponding to the beginning of mode oscillation and whose amplitude is altered by scope sampling, three detection levels appear that correspond to the different modes involved in this regime. The order of appearance of the modes starting from the lowest intensity mode 1 is then 12321.

By means of the fine-tuning of the cavity length, it is possible to activate simultaneously the $q = 4$ family and the TEM_{00} mode, as the transverse spacing is 17 MHz because each mode is able to oscillate in a typical frequency range of 40 MHz. Therefore these modes oscillate with longitudinal indices differing by one unit. In these conditions, when the laser is operated in the absence of saturable absorber, the time averaged pattern as displayed by the thermal plate without saturable absorber clearly results from the superposition of several modes [see Fig. 10(a)]. When the SF_6 pressure is set in the multistability domain, the saturable absorber acts as a mode-selector and the laser delivers patterns very similar to pure modes of the empty cavity. Here due to the asymmetry of the cavity mainly imposed by the Brewster windows and the grating, the modes resemble Hermite–Gauss modes. In this case shown in Fig. 10(b), these are the $TEM_{1,3}$, $TEM_{3,1}$ and $TEM_{0,0}$ modes and so multistability between three transverse modes is obtained. For a given set of experimental parameters, which mode is selected depends only on the initial conditions. This multistability is a very general feature which stays as the Fresnel number is increased. For instance, when the Fresnel number is fixed to $N = 10$, the modes of the family whose transverse index q lies between $q = 0$ and 5 can oscillate when they are brought close to the centre of the gain curve. When the cavity length is steadily increased over half a wavelength in such a way that the above-mentioned families are successively in resonance, multistability

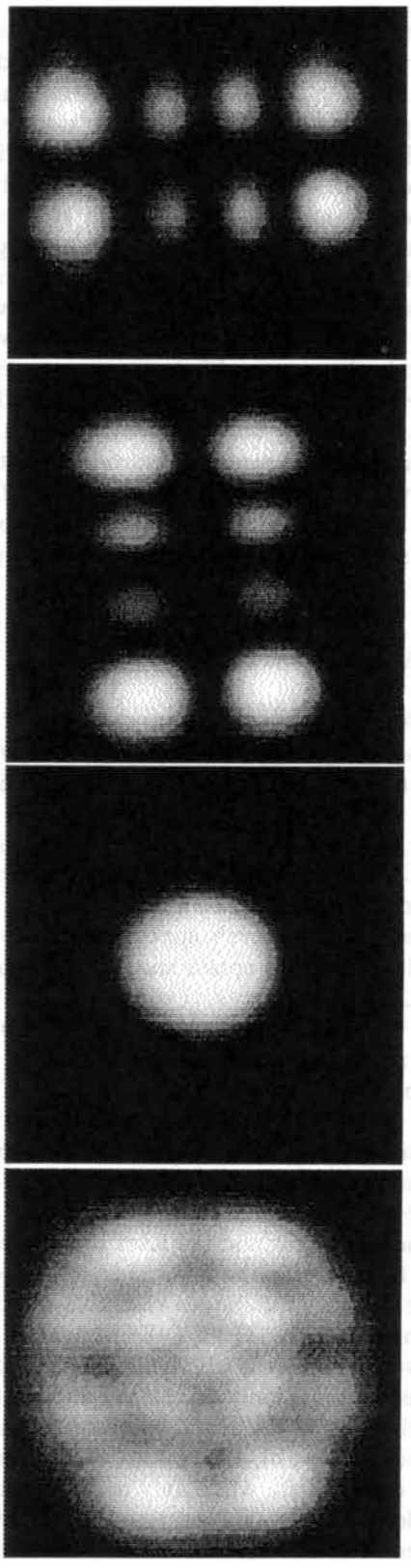

Fig. 10. Multistability between the $q = 0$ and 4 families obtained at $N = 10$. (a): Pattern without absorber, (b)–(d): multistable stationary states in the presence of absorber.

involving a large number of states has been obtained. Figure 11 reports the domains of existence of each of the modes of the families with $q \leqslant 4$ as a function of the cavity length. Each mode appears on a certain range of cavity length, typically of the order of $\lambda/4$, resulting in a frequency tuning range of about 45 MHz, and each family is shifted with respect to the previous one by about 30 MHz. Note that in these experiments, the asymmetry was rather large, resulting in a degeneracy lift of the modes of the same family of the order of 10 MHz. This figure shows that multistability between up to 10 different transverse patterns is commonly achieved. Note that contrary to the bimode situation, multistability is observed not only between modes of a given family but also between modes belonging to different q families.

When the cavity having a large Fresnel number $N = 37$ is used instead of the previous one, the number of stable states is much increased and Hermite–Gauss states with large transverse dimensions may be selected by the absorber. Figure 13 gives some samples of

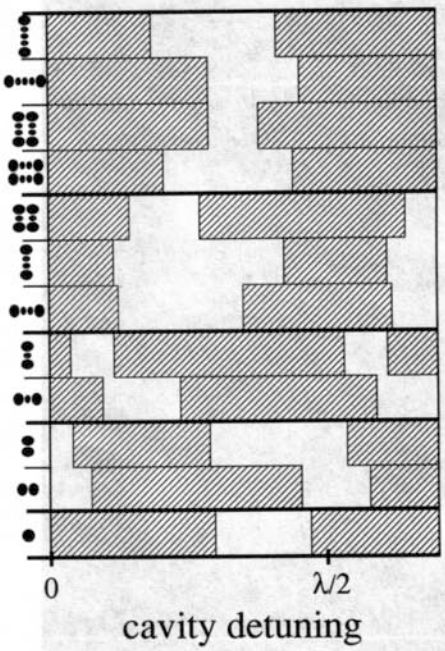

Fig. 11. Multistability diagram as a function of the cavity length. Each mode is stable in the hatched region.

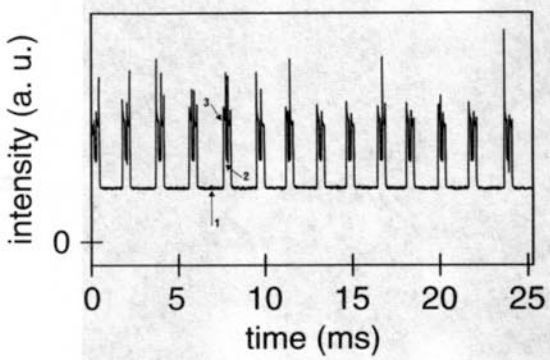

Fig. 12. Time evolution of the output intensity of the laser in a regime of periodic alternance involving three modes. 1, 2 and 3 refer to the detected level of each mode.

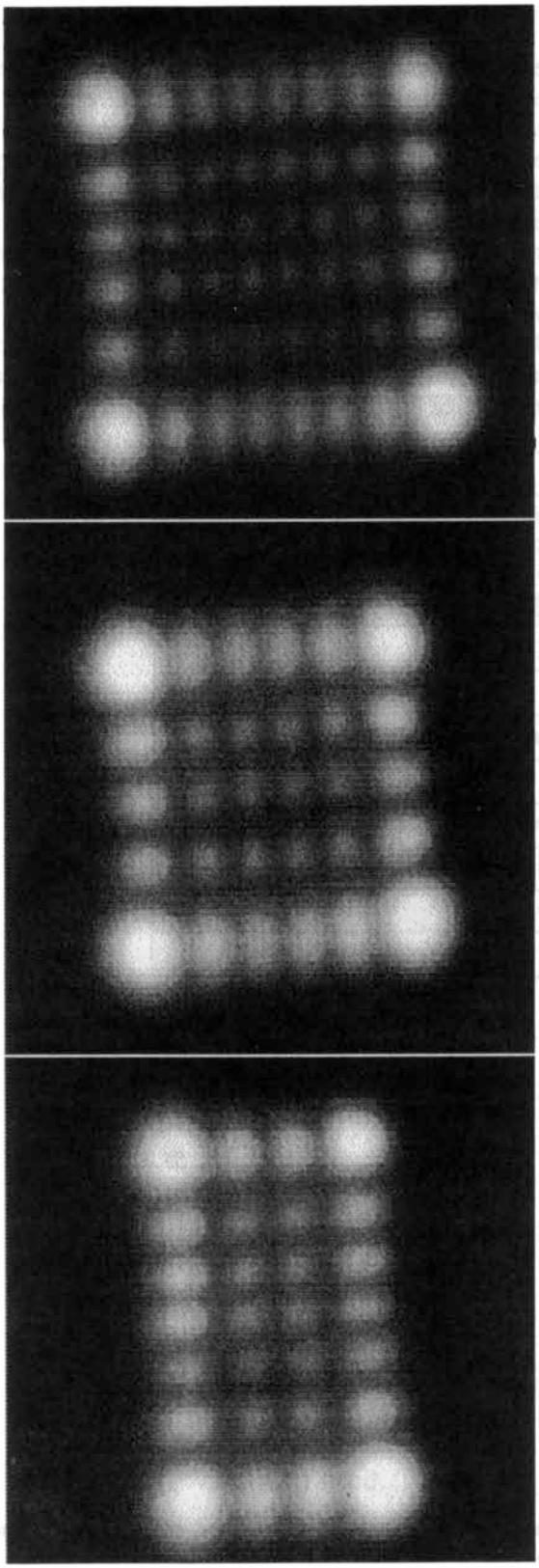

Fig. 13. Mode filtering at large Fresnel number ($N = 37$) with $P_{abs} = 12$ mTorr. (a) $q = 9$ family, mode TEM_{36}, (b) $q = 9$ family, mode TEM_{54}, (c) $q = 12$ family, mode TEM_{75}.

the patterns, for example, modes of the $q = 9$ and $q = 12$ families observed in these conditions. In addition to this multistable behaviour, the multimode LSA also exhibits PQS with simultaneous oscillations of several modes and periodic alternance. Three mode oscillation will be discussed later in the case of PQS and periodic alternance.

CONCLUSION

Experiments on the $CO_2 + SF_6$ LSA have shown that the saturable absorber placed inside the laser cavity strongly modifies the transverse patterns of a multimode laser. In particular, one of the most spectacular properties of the system is its spatial multistable behaviour that could be monitored by optical switching. Local modulation in the millisecond time-scale of the different part of the pattern has been obtained via regimes of periodic and irregular alternance. The analysis of the bimode case has allowed several cases of simple dynamics of the system to be cleared out and will provide the basis for the analysis of the largely multimode case which is now in progress.

Acknowledgement—This work is carried out under DRET convention No. 92101.

REFERENCES

1. M. Lefranc, D. Hennequin and D. Dangoisse, Homoclinic chaos in a laser containing a saturable absorber, *J. Opt. Soc. Am.* **B8**, 239–249 (1991).
2. D. Hennequin, F. de Tomasi, B. Zambon and E. Arimondo, Homoclinic orbits and cycles in the instabilities of a laser with saturable absorber, *Phys. Rev.* **A37**, 2243–2246 (1988).
3. B. Zambon, Theoretical investigations of models for the laser with a saturable absorber: a case of homoclinic tangency to a periodic orbit, *Phys. Rev.* **A44**, 688–702 (1991).
4. E. Arimondo, F. Casagrande, L. Lugiato and P. Gloricux, Repetitive passive Q-switching in lasers with saturable absorbers, *Appl. Phys.* **B30**, 57–77 (1983).
5. A. G. Kagan and Ya. I. Khanin, Problems in steady-state theory of a multimode laser with a selective saturable absorber, *Sov. J. Quantum Electron.* **13**, 88–92 (1983).
6. V. P. Chebotaev, I. M. Beterov and V. N. Lisitsyn, Selection and self-locking of modes in a He–Ne laser with nonlinear absorption, *IEEE J. Quant. Electron.* **4**, 788–790 (1968).
7. *Transverse Effects in Nonlinear Optical Systems*, edited by N. B. Abraham and W. J. Firth, Special Issue, *J. Opt. Soc. Am.* **B5** (1990).
8. M. Brambilla, F. Battipede, L. A. Lugiato, V. Penna, F. Prati, C. Tamm and C. O. Weiss, Transverse laser patterns, *Phys. Rev.* **A43**, 5090–5113 (1991).
9. C. Tamm and C. O. Weiss, Bistability and optical switching of spatial patterns in a laser, *J. Opt. Soc. Am.* **B7**, 1034–1038 (1990).
10. C. O. Weiss, Spatio-temporal structures—II. Vortices and defects in lasers in Quantum Optics, *Proc. XXth Solvay Conf.*, edited by P. Mandel, *Phys. Rep.* **219**, 311–338 (1992).
11. F. T. Arecchi, G. Giacomelli, P. L. Ramazza and S. Residori, Experimental evidence of chaotic itinerancy and spatio-temporal chaos in optics, *Phys. Rev. Lett.* **65**, 2531–2534 (1990).
12. S. R. Liu and G. Indebetouw, Periodic and chaotic spatiotemporal states in a phase-conjugate resonator using a photorefractive $BaTiO_3$ phase-conjugate mirror, *J. Opt. Soc. Am.* **B9**, 1507–1520 (1992).
13. J. R. Tredicce, E. J. Quel, A. M. Ghazawi, C. Green, M. A. Pernigo, L. M. Narducci, and L. A. Lugiato, Spatial and temporal instabilities in a CO_2 laser, *Phys. Rev. Lett.* **62**, 1274–1277 (1989).
14. M. Sargent III, M. O. Scully and W. E. Lamb, *Laser Physics*. Addison-Wesley, New York (1974).
15. I. M. Belousova, G. N. Vinokurov, O. B. Danilov and N. N. Rosanov, Mode interaction in a gas laser with spherical mirror resonators, *Sov. Phys. JETP* **25**, 761–767 (1967).
16. D. H. Auston, Transverse mode locking, *IEEE J. Quant. Electron.* **4**, 471–473 (1968).
17. P. W. Smith, Simultaneous phase-locking of longitudinal and transverse laser modes, *Appl. Phys. Lett.* **13**, 235–237 (1968).
18. D. Hennequin, D. Dangoisse and P. Glorieux, Farey hierarchy in a bimode CO_2 laser with a saturable absorber, *Phys. Rev.* **A42**, 6966–6968 (1990).
19. D. Hennequin, D. Dangoisse and P. Glorieux, Instabilities in a bimode CO_2 laser with a saturable absorber, *Opt. Commun.* **79**, 200–206 (1990).
20. V. Yu. Kurochin, A. N. Rurukin, V. N. Petrovsky, E. D. Protsenko, V. M. Yermanenko and A. M. Golovchenko, Emission dynamics of a double mode CO_2 laser with an intracavity saturable absorber, *Opt. Commun.* **95**, 165–172 (1993).

21. M. Tachikawa, F. L. Hong, K. Tanii and T. Shimizu, Deterministic chaos in passive Q-switching pulsation of a CO_2 laser with saturable absorber, *Phys. Rev. Lett.* **60**, 2266–2268 (1988).
22. M. Tachikawa, K. Tanii and T. Shimizu, Laser instability and chaotic pulsation in a CO_2 laser with intracavity saturable absorber, *J. Opt. Soc. Am.* **B5**, 1077–1081 (1988).
23. J. Testa, Fractal dimension at chaos of a quasiperiodic driven tunnel diode, *Phys. Lett.* **A111**, 243–245 (1985).
24. L. Glass, M. R. Guevara, A. Shrier and R. Perez, Bifurcation and chaos in a periodically stimulated cardiac oscillator, *Physica* **D7**, 89–101 (1983).
25. J. C. Roux, R. H. Simoyi and H. L. Swinney, Observation of a strange attractor, *Physica* **D8**, 257–266 (1983).
26. A. Barsella, P. Alacantara Jr, E. Arimondo, M. Brambilla and F. Prati, Dynamics of transverse patterns in a laser with saturable absorber: model and numberical analysis, *Chaos, Solitons & Fractals* **4**, 1665–1682.
27. D. Hennequin, C. Lepers, E. Louvergneaux, D. Dangoisse and P. Glorieux, Spatio-temporal dynamics of a weakly multimode CO_2 laser, *Opt. Commun.* **93**, 318–322 (1992).